



# An Experimental Application of Four Types of Chitosan Bead for Removal of Cationic and Anionic Pollutants

Byungryul An · Jae-Woo Choi

Received: 15 September 2019 / Accepted: 5 December 2019 / Published online: 14 December 2019  
© Springer Nature Switzerland AG 2019

**Abstract** Four types of chitosan bead (CB) were tested to find the removal efficiency for cation and anion from solution. Hydrogel chitosan bead (HCB) was first prepared and then modified by chemical and physical treatment. Both the Cu(II) and phosphate removal were investigated based on the batch removal efficiency, a pH test, kinetics, and an isotherm test. For Cu(II) application, the highest Cu(II) uptake (approximately 83%) was obtained for the HCB; the modification by crosslinking by glutaraldehyde (GA) and air drying decreased this to approximately 60%, while phosphate removal was not affected by crosslinking and drying. Below pH 4.0, the removal efficiency of Cu(II) was decreased by approximately 20% for all type of CB, while phosphate uptake was determined by the type of CB, regardless of the initial pH. The maximum Cu(II) and phosphate uptake ( $Q$ ) were 129 and 232 mg/g for the HCB and dried chitosan bead (DCB), respectively. The phosphate sorption rate was faster than Cu(II) at the

beginning of the reaction for the hydrogel bead, while the dried bead reached the equilibrium in 72 h.

**Keywords** Adsorption · Amino group · Chitosan bead · Cu(II) · Phosphate

## 1 Introduction

Heavy metals, such as cadmium, copper, nickel, and lead, and anions, such as sulfate, phosphate, and chloride, are naturally present as water contaminants (Hu and Cheng 2013; Wu et al. 2015). In general, the presence of heavy metals in a solution would cause fatal damage to humans through long-term intake. For example, Cu(II), a widely used metal as electronic industries are growing rapidly, is released into water bodies at concentrations of up to 100 mg/L, causing nausea, vomiting, and stomach cramps for humans and aquatic organisms (Sorvari and Sillanpää 1996; Jo et al. 2012).

Among the anions, phosphorus is a critical nutrient of algal blooms and is considered to be one of the core contaminants that cause eutrophication (Schindler 1974; An et al. 2014a). The effluent concentration of phosphorus discharged from domestic, agricultural, and industrial wastewater should be controlled (Conley et al. 2009). For example, the maximum concentration of phosphorus was legislated in the USA (USEPA 1986) and Korea (Kim et al. 2018).

To remove or enhance the removal of Cu(II) or phosphorus, the following technologies have been studied: chemical precipitation (Sampaio et al. 2009),

B. An  
Department of Civil Engineering, Sangmyung University,  
Cheonan, Chungnam 31066, Republic of Korea

J.-W. Choi  
Water Cycle Research Center, Korea Institute of Science and  
Technology, Hwarang-ro 14-gil 5, Seongbuk-gu, Seoul 02792,  
Republic of Korea

J.-W. Choi (✉)  
Division of Energy & Environment Technology, KIST School,  
Korea University of Science and Technology, Seoul 02792,  
Republic of Korea  
e-mail: plead36@kist.re.kr

membranes (Denizli et al. 2000), and ion exchange (IX) (Cegłowski et al. 2018). Although each method has distinct advantages as they may be cost-effective, have a high removal efficiency, and are easily operated, respectively, there are drawbacks, such as high levels of sludge production, the requirement of high operation and maintenance costs, and low selectivity towards the target contaminant for chemical precipitation, membrane, and ion exchange, respectively.

As the interest in the simultaneous removal of both cations and anions has increased, many studies have been conducted on a variety of materials. Shah and Chudasama (2014) developed a hybrid chelating ion exchanger using zirconium oxychloride and diethylenetriamine (DETA), which remove both Cu(II) and chloride. Zeolite synthesized from fly ash (Liu et al. 2018) and impregnated with NaOH-lanthanum (He et al. 2016) was studied for removing ammonium ( $\text{NH}_4^+$ ) and phosphate ( $\text{PO}_4^{3-}$ ). Mesoporous silica (MS) modified via amino group post-grafting and synthesized using a melamine-based dendrimer group has been used in the removal of Pb(II) and nitrate ions (Chen et al. 2015) and Cu(II) and sulfate (Wu et al. 2015), respectively.

Based on previous studies, creating a new functional group is required to simultaneously remove pollutants from a solution. However, some biopolymers, such as alginate, glucose (Stoll and Duncan 1996), and chitosan, which were functionalized with carboxyl, aldehyde, and amino groups, respectively, have been used in the field of water and wastewater treatment as adsorbents offering non-toxicity, high reactivity, and cost-effectiveness. Among them, chitosan has received increased interest owing to the properties provided by the amino functional group. Chitin and chitosan were first investigated in the field of medicine as they are non-toxic to humans in their various forms, including nanoparticles (Wang et al. 2011), membranes (Thakur and Voicu 2016), sponges (Noel et al. 2010), and fibers (Pillai et al. 2009). Lately, chitin and chitosan have been used as beads to remove target contaminants during the adsorption process.

Hydrogel chitosan bead (HCB) was first used to directly remove heavy metals (Zhao et al. 2007) and anions such as arsenic (Malwal and Gopinath 2017). However, due to its drawbacks, such as their weak physical hardness and unstable chemical composition at low pH, HCB was modified by drying and crosslinking to increase its physical and chemical strength, respectively, resulting in increased application

in water and wastewater treatment (Liu and Zhang 2015). However, only the removal of a single target contaminant has been reported, and the bifunctional removal of cations and anions with the effect of physical and chemical modification has not.

The overall goal of this study was to investigate the effect of drying and employing a crosslinking agent on the simultaneous sorption capacity for Cu(II) and phosphate. The specific objectives were to (1) prepare hydrogel chitosan bead and treat by drying and crosslinking; (2) determine the change in physical and chemical properties; (3) investigate the sorption capacity for Cu(II) and phosphate by batch tests, sorption isotherms, and sorption kinetics; and (4) evaluate the possible sorption mechanism from the effect of drying and crosslinking for simultaneous removal.

## 2 Materials and Methods

### 2.1 Chemicals

Chitosan powder with a medium molecular weight of  $\sim 250,000$  g/mol and a 75–85% degree of deacetylation from chitin was purchased from Sigma-Aldrich (USA). The GA solution (25 wt.%) was obtained from SHOW (Tokyo, Japan). The chemicals of  $\text{KH}_2\text{PO}_4$ ,  $\text{CuCl}_2 \cdot 2\text{H}_2\text{O}$ , HCl, and NaOH were also obtained from Sigma-Aldrich (USA) and used without further purification.

### 2.2 Preparation of CB

The preparation of CB has been documented by various studies (Guibal et al. 1998; An et al. 2014a). A previous study (An et al. 2014a) suggested the optimized initial conditions, such as concentration of chitosan and acid solution, for maintaining the physical form during preparation. In brief, a 2.5% (*w/w*)-chitosan solution was first prepared by adding 10 g of chitosan flakes into 400 g of a 1% HCl solution and stirring for at least 12 h at room temperature (approximately 21 °C). To note, a higher temperature should not be used to increase the dissolution rate. The chitosan solution was then dropped into 400 mL of 1 M NaOH with mild stirring. After this, the mixed solution was left for over 24 h, and then washed with DI until the pH was 7.5–8, and this was denoted as the hydrogel chitosan bead (HCB).

To increase the chemical stability, the HCB was mixed with 0.5 M of glutaraldehyde (GA) solution (400 mL) for at least 24 h, and the mixture was washed with DI (HCB-G). After preparing the HCB and HCB-G, both beads were dried in air until the mass no longer changed. These beads are referred to as DCB and DCB-G, respectively.

### 2.3 Physical and Chemical Characterization

Physical properties, such as the mean diameter (mm), water content (%), and degree of swelling (%), were measured for four CBs using 400 samples. The water content was measured after drying at 60 °C, and the degree of swelling of DCB and DCB-G was calculated based on the change in the total volume.

Fourier transform infrared spectroscopy (FTIR) spectra (LUMOS, Bruker, Germany) were employed to determine the crosslinking interactions and Cu(II) and phosphate sorption mechanisms in a wavenumber range of 540 to 4000  $\text{cm}^{-1}$  for five representative samples.

### 2.4 Batch Sorption Test

To investigate the Cu(II) and phosphate removal efficiencies, a series of batch tests were conducted using the CBs. The initial concentrations of Cu(II) and phosphate in the 50-mL mixture were 20 and 30 mg/L, respectively, which is the equimolar ratio. Each sample was then rotated at 10 rpm for 96 h. The following batch tests were initiated with the same initial concentrations of Cu(II) and phosphate. The solution pH is a critical parameter to determine the removal capacity of an adsorption process. Therefore, a batch test was conducted at different initial solution pH values of 3.86, 4.34, and 5.08 with phosphate, and they were rotated for 96 h.

To determine the sorption rates of Cu(II) and phosphate, batch kinetic tests were conducted for the four CB. The initial concentrations of Cu(II) and phosphate were set to 20 and 30 mg/L, respectively, and the tests were initiated by adding a desired weight of beads into a 300-mL glass bottle. The samples were agitated on a shaker and an aliquot was collected at predetermined intervals. The initial pH was not adjusted during the tests and was monitored.

Sorption isotherm tests were performed for four CB to determine their sorption capacity for both Cu(II) and phosphate. A desired amount of CB was mixed with 50 mL of the solution in a Falcon tube. The mixtures

were rotated at 10 rpm for 96 h. The initial pH was set to 5.0 and the final pH was monitored. The uptake value based on the mass balance for Cu(II) and phosphate was obtained from the following equation:

$$q_e = \frac{V(C_0 - C_e)}{M} \quad (1)$$

where  $q_e$  is the equilibrium mass uptake of Cu(II) or phosphate with a sorbent (mg/g),  $V$  is the solution volume (L),  $C_0$  and  $C_e$  are the initial and final concentrations of Cu(II) and phosphate in the solution, respectively (mg/L), and  $M$  is the mass of the added sorbent (g).

### 2.5 Chemical Analyses

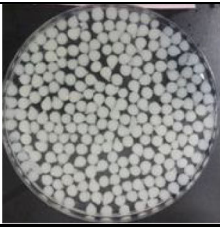
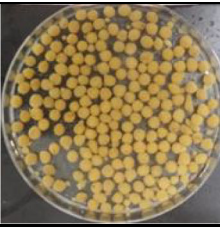
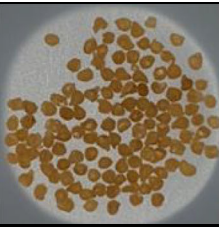

The solution pH was measured using an ORION Star A211 (Thermo Scientific, USA). The concentrations of Cu(II) and phosphate (as phosphorus) were analyzed using inductively coupled plasma (ICP) spectroscopy (Model: NexION 300D, Agilent Technologies, USA) or a Laboratory VIS Spectrophotometer (Model: DR 3900, HACH, USA) for Cu(II) and Potable analyzer (Model: HS-1000plus, HUMAS, Korea) for phosphorus.

## 3 Results and Discussion

### 3.1 Characteristics of Chitosan Bead

Table 1 is created using a photograph and the salient properties of four types of CB, i.e., HCB, HCB-G, DCB, and DCB-G, which were differentiated with the addition of GA as a crosslinking agent and air drying. According to the photograph in Table 1, both hydrogel beads (HCB and HCB-G) appear to be more spherical than the dried bead (DCB and DCB-G). After the HCB was crosslinked, the color changed from white to yellow, and after air drying, HCB and HCB-G became translucent and dark brick-red in color, respectively (Monteiro Jr. and Airoidi 1999). The highest bead size (mm) of 4.69 mm was obtained for HCB, followed by 4.38, 1.47, and 1.21 mm for HCB-G, DCB, and DCB-G, respectively. The weight of CB was 27.4, 26.3, 1.18, and 1.38 g/400 ea for HCB, HCB-G, DCB, and DCB-G, respectively. The water contents of HCB and HCB-G were 95.7 and 94.7%, respectively.

**Table 1** Salient properties of the chitosan beads (average  $\pm$  standard deviation)

	HCB	HCB-G	DCB	DCB-G
Photographic				
Diameter <sup>a</sup> , mm	4.69 $\pm$ 0.0369	4.38 $\pm$ 0.0370	1.47 $\pm$ 0.206	1.21 $\pm$ 0.124
Weight <sup>a</sup> , g	27.4 $\pm$ 0.981	26.3 $\pm$ 0.464	1.18 $\pm$ 0.00707	1.38 $\pm$ 0.0113
Water content, %	95.7 $\pm$ 0.180	94.7 $\pm$ 0.0497	-	-
Degree of swelling, %	-	-	252 $\pm$ 3.09	86.2 $\pm$ 4.01

<sup>a</sup> Measured for 400 samples

<sup>a</sup> Measured for 400 samples

Based on the results in Table 1, the variation rate (%) of the diameter and weight was calculated and is presented in Table 2 to determine the effects of crosslinking and air drying. Crosslinking by GA did not cause a significant physical change (less than 10% reduction in diameter and weight), although the tendency of diameter and weight is reduced by adding GA to the hydrogel beads. However, when comparing DCB with DCB-G, the weight was increased by approximately 17% due to the interaction of GA with the chitosan polymer, and the diameter was decreased by approximately 17%. The smaller size and water contents of HCB-G and DCB-G could be attributed to the exclusion of water molecules from the chitosan

polymer chain during crosslinking, leading to interactions among the amino groups (An et al. 2014a). In addition, the chromatography of hydrophobic interactions was studied on chitosan (Agarwal and Gupta 1995).

The swelling rate (%) in water can indirectly reveal the chemical interactions between water and the chitosan polymer. Values of 252.9 and 86.2% by volume were obtained for DCB and DCB-G, respectively, indicating that both dried bead was not recovered fully and their hydrophilicities were changed by drying. Moreover, the lower degree of swelling for DCB-G also indicates that GA influences chemical interactions between the chitosan polymer chain and GA.

**Table 2** Comparison of the variations (%) in diameter and weight

Crosslinking	Diameter		Weight		
	Diameter	Weight	Diameter	Weight	
HCB vs HCB-G	-6.54	-3.98	HCB vs DCB	-64.3 <sup>b</sup>	-95.6
DCB vs DCB-G	-17.7	+17.0 <sup>a</sup>	HCB-G vs DCB-G	-72.4	-94.7

<sup>a</sup> Positive indicates that the value decreased

<sup>b</sup> Negative indicates that the value increased

### 3.2 FTIR

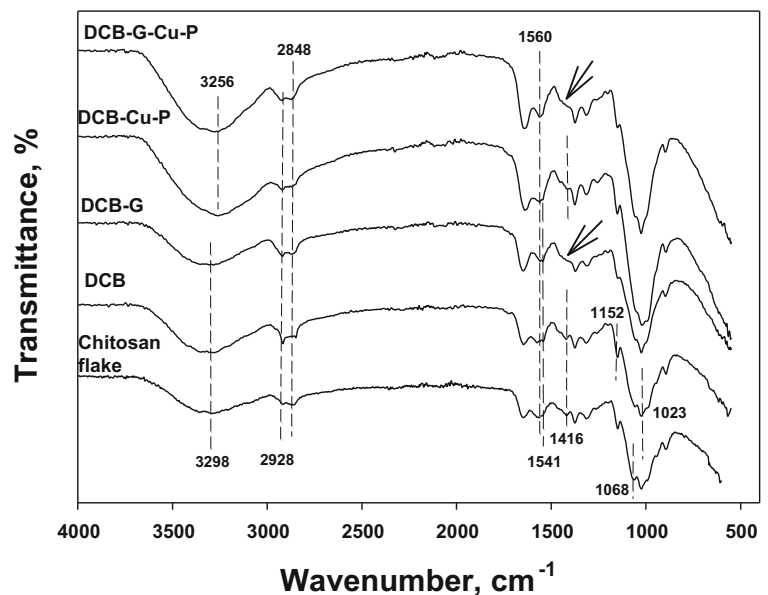
Chemical bonding for the chitosan flakes, DCB, DCB-G, DCB-Cu(II) + phosphate, and DCB-G-Cu(II) + phosphate was identified by FTIR spectra ranging from 540 to 4000  $\text{cm}^{-1}$ , as shown in Fig. 1. The broad band ranging from 3000 to 3500  $\text{cm}^{-1}$  for all samples was assigned to the stretching vibration of O–H at 3354  $\text{cm}^{-1}$  and N–H at 3286  $\text{cm}^{-1}$  from the water and chitosan polymer, respectively (Modrezejewska 2013). In comparison with the chitosan flake, after synthesizing the bead (DCB and DCB-G), the peak intensity at 3298  $\text{cm}^{-1}$  decreased. Finally, the peak was overlapped and shifted to approximately 3256  $\text{cm}^{-1}$  after the sorption of Cu(II) and phosphate. The shift was monitored by Modrezejewska (2013) and An et al. (2014a), who stated that the chelating complexes between the amino group and Cu(II) or phosphate were formed after sorption. The bands at 2928 and 2848  $\text{cm}^{-1}$  corresponded to the symmetric and asymmetric stretching of C–H, respectively (Queiroz et al. 2015). The carbonyl group (C=O) in the chitosan polymer presented a peak at 1648  $\text{cm}^{-1}$  (Li et al. 2013). Previous studies indicated that the peaks at approximately 1571 and 1543  $\text{cm}^{-1}$  can be attributed to  $\text{NH}_2$  and  $\text{NH}_3^+$ , respectively, and, moreover, the disappeared or weakened peak at approximately 1543  $\text{cm}^{-1}$  was due to the transformation of  $\text{NH}_3^+$  into  $\text{NH}_2$  caused by interactions (Osman and Arof 2003; Xie et al. 2009). Therefore, in this study, the peaks at

1560 and 1541  $\text{cm}^{-1}$  were assigned to the amino group, and a weakened peak at 1541  $\text{cm}^{-1}$  was observed after sorption. The peak at 1416  $\text{cm}^{-1}$  disappeared for DCB-G and DCB-G-Cu(II)-P, which can be explained by the effect of GA on the N–H bonds from primary amines (Jabli et al. 2011). The peaks at 1068 and 1023  $\text{cm}^{-1}$  indicated C–O stretching, and C–O–C bridge stretching was observed at 1152  $\text{cm}^{-1}$  (Osman and Arof 2003).

### 3.3 Removal Efficiency

Batch experiments were conducted for four types of CB to determine the removal efficiency of Cu(II) and phosphate, as shown in Fig. 2. The removal efficiencies of both Cu(II) and phosphate are presented on the left y-axis. The highest Cu(II) removal efficiency for HCB was approximately 83%, which decreased to approximately 59% and 34% for HCB-G = DCB and DCB-G, respectively. The phosphate removal efficiency decreased in the following order: DCB (70%) > HCB-G = DCB (60%) > DCB-G = HCB (35%). The decrease in the removal efficiencies of HCB was from 87% for Cu(II) to 35% for phosphate, while all the other CBs exhibited similar Cu(II) and phosphate removal efficiencies. To determine the removal capacity of each CB, the total amounts of Cu(II) and phosphate in mmol were added to the right y-axis. This released a similar total removal capacity, ranging from 0.018 to 0.020, for HCB, HCB-G, and DCB, in spite of the fluctuating removal

**Fig. 1** FTIR spectra of the chitosan flakes, DCB, DCB-G, DCB with Cu(II) + phosphate, and DCB-G with Cu(II) + phosphate



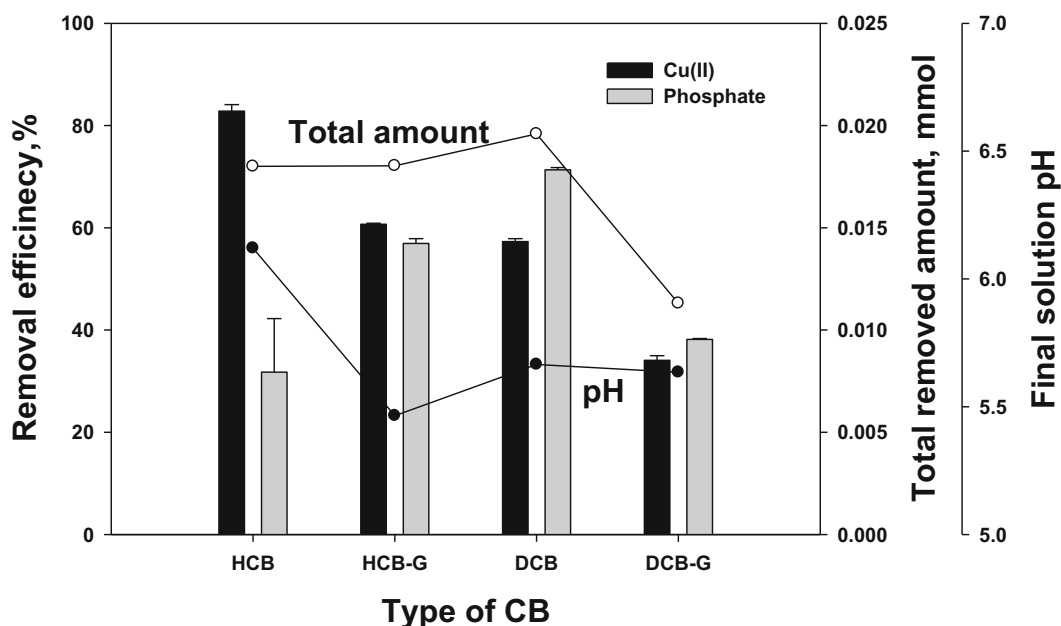


**Fig. 2** Removal efficiency of Cu(II) and phosphate (left y-axis), the total removed amount, and final solution pH (right y-axis) for the different CBs

efficiency of HCB. The application of DCB-G only gained 0.010 mmol in total, which was an approximate reduction of 58% compared to the other CB.

Some studies reported that the addition of GA to chitosan as a crosslinking agent can reduce the sorption capacity due to the loss of the amino functional group in the chitosan polymer by the reaction with the carbonyl group of GA (Kildeeva et al. 2009; Ishii et al. 1997), and Wan Ngah (2002) observed an approximate decrease in Cu(II) of 25%. However, this result showed that the decreased Cu(II) uptake leads to an increase in the phosphate uptake, and the total capacity did not differ between the type of hydrogel. Poon et al. (2014) suggested that a highly crosslinked homopolymer could be produced by the self-polymerization of GA. As a result, the absorbable site of CB was not reduced, and the effect of GA on the sorption capacity is negligible. Meanwhile, crosslinking significantly affects the removal capacity of the dried bead.

The different phenomena for the HCB can be explained by the shift in internal pH. The calculated  $pK_a$  value of chitosan determined by the degree of deacetylation (DD) and molecular weight (M.W) was 6.5 (Wang et al. 2006); therefore, the amino group was deprotonated from  $NH_2$  to  $NH_3^+$  above this  $pK_a$  value, resulting in an increased affinity for Cu(II) associated with  $NH_2$ . Therefore, at the highest final pH, HCB has

higher affinity for Cu(II) over phosphate than the other CB.

The reduction in the capacity of DCB-G is due to its physical properties. From Table 1, DCB-G was smaller than DCB, but its weight was higher, indicating a higher density. In addition, the swelling rate of DCB-G is below that of DCB. Therefore, the accessibility of ions was restricted in the denser polymer network by crosslinking and drying.

### 3.4 pH Effect

The solution pH is a critical parameter in determining the sorption capacity due to the speciation of both Cu(II) and phosphate, and surface charge of the sorbent. Moreover, the protonation/deprotonation occurring in the amino group of the chitosan polymer is also an independent parameter of the sorption capacity. Equation (2) illustrates the protonation and deprotonation.

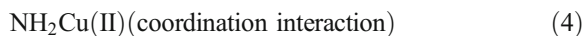
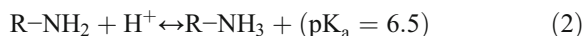


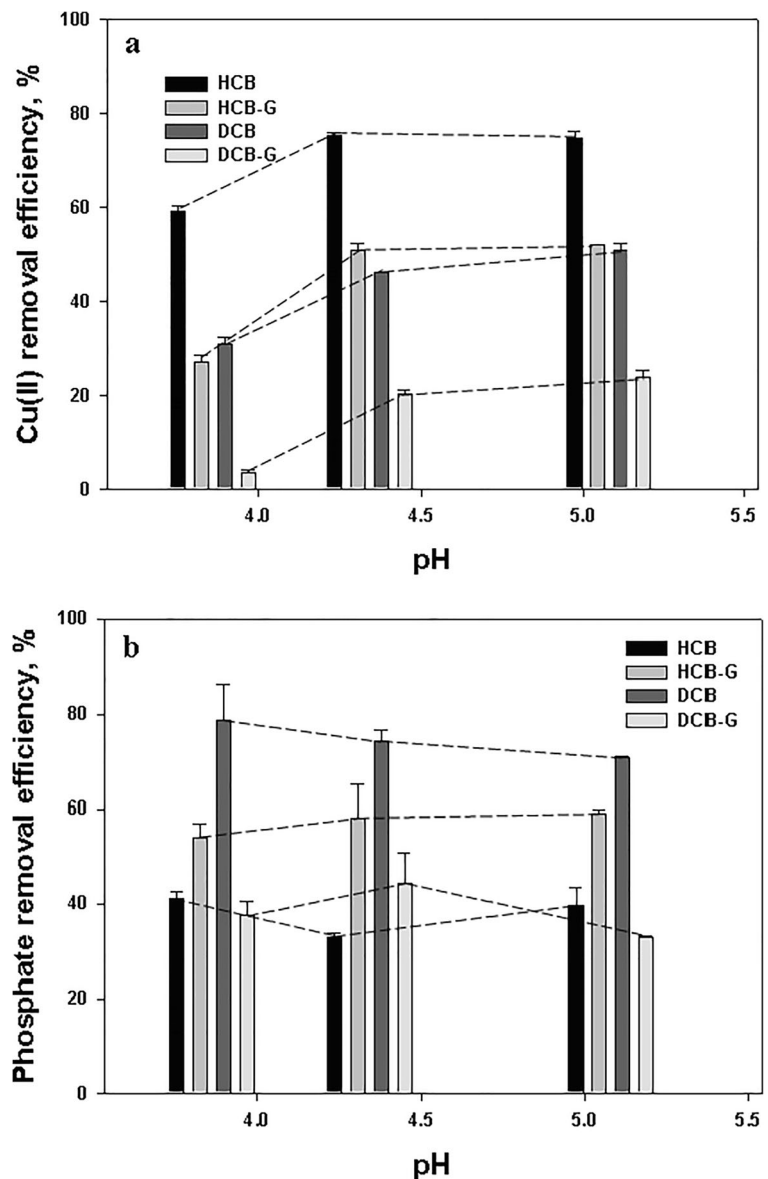
Figure 3 shows the Cu(II) and phosphate removal efficiencies at initial pH of 3.86, 4.34, and 5.08. At pH 3.86, the Cu(II) removal efficiency was reduced by approximately 20% at pH 4.34 and 5.08, and no change in the sorption capacity was found at 4.34 and 5.08 for all CBs. This result agrees with that of Zhao et al. (2007) for HCB-G and Verbych et al. (2005) for HCB. This could be due to the effect of hydrogen and deprotonation of the amino group. At a low pH, Cu(II) competes with high concentrations of hydrogen ions and the ratio of  $\text{NH}_3^+$  in the amino group of the chitosan polymer increased, based on Eq. (2). Therefore, both forces reduce

the Cu(II) sorption capacity and available sorption sites, respectively.

Based on Eqs. (2)–(4) and the  $\text{pK}_a$  value of chitosan, coordination interactions were rarely involved in the sorption of Cu(II) under the current pH conditions. To explain the mechanism of Cu(II) sorption, previous studies stated that the oxygen in the chitosan polymer chain can take part in removing cations (Domard 1987). However, sorption is due to the inner hydroxide effect, resulting in the gap between the apparent and real pH.

In contrast, the removal of phosphate was less sensitive to the solution pH than that of Cu(II). Rajeswari

**Fig. 3** Cu(II) (a) and phosphate (b) removal efficiencies as a function of pH for the different CBs



et al. (2015) observed a similar result between pH 3 and 5. According to the Katchalsky equation (Xie et al. 2009), which gives the degree of dissociation ( $\alpha$ ) as a function of pH at a given  $pK_a$ , as shown in Fig. 4, the value of  $\alpha$  increases with a decrease in pH and reached 1.0 at pH 4, regardless of the suggested values of  $pK_a$ . Most amino groups formed as the  $NH_3^+$  functional group. Under the current pH (3–5), the  $H_2PO_4^-$  species exceed 90% ( $pK_{a1} = 2.1$   $pK_{a2} = 7.2$ ). Therefore, the electrostatic interactions between  $NH_3^+$  and  $H_2PO_4^-$  are a predominant force for the removal of phosphate (Eq. (3)).

### 3.5 Isotherm Test

The equilibrium sorption date (symbol) for Cu(II) and phosphate was fitted by the classical Langmuir model (Eq. (4)) to investigate and compare the maximum sorption capacities. The simulated value (solid line) is shown in Fig. 5, and the values of Langmuir parameter calculated from the fitted model are listed in Table 3.

$$q_e = \frac{bQC_e}{1 + bC_e} \quad (5)$$

where  $q_e$  is the equilibrium Cu(II) and  $PO_4$  uptake (mg/g),  $C_e$  is the equilibrium concentration of Cu(II) in the

aqueous phase (mg/L),  $Q$  is the maximum capacity for Cu(II) and phosphate (mg/g), and  $b$  (L/mg) is the Langmuir affinity coefficient between the chitosan bead and Cu(II) and phosphate.

HCB achieved the highest and lowest  $Q$  for Cu(II) and phosphate, which confirmed the batch removal efficiency for the cation and anion, respectively, while the shape and calculated value of  $Q$  of the other three CBs for Cu(II) and phosphate were similar. Wan Ngah et al. (2002), who used GA, ECH, and EGDE as crosslinking agents for only Cu(II), showed that the crosslinking agent reduced the maximum Cu(II) sorption capacity by 22–43%, and Poon et al. found that the increased amount of crosslinking agent enhanced the sorption capacity for p-nitrophenol. The crosslinking agent can increase the positive zeta potential (Chang et al. 2008), resulting in an increase in anions and decrease in cations.

### 3.6 Kinetic Test

The adsorption rates of Cu(II) and phosphate for all CB are shown in Fig. 6. The sorption equilibrium for Cu(II) was reached at 50 h for HCB and 72 h for HCB-G and DCB, while sorption still continued after 72 h for DCB-

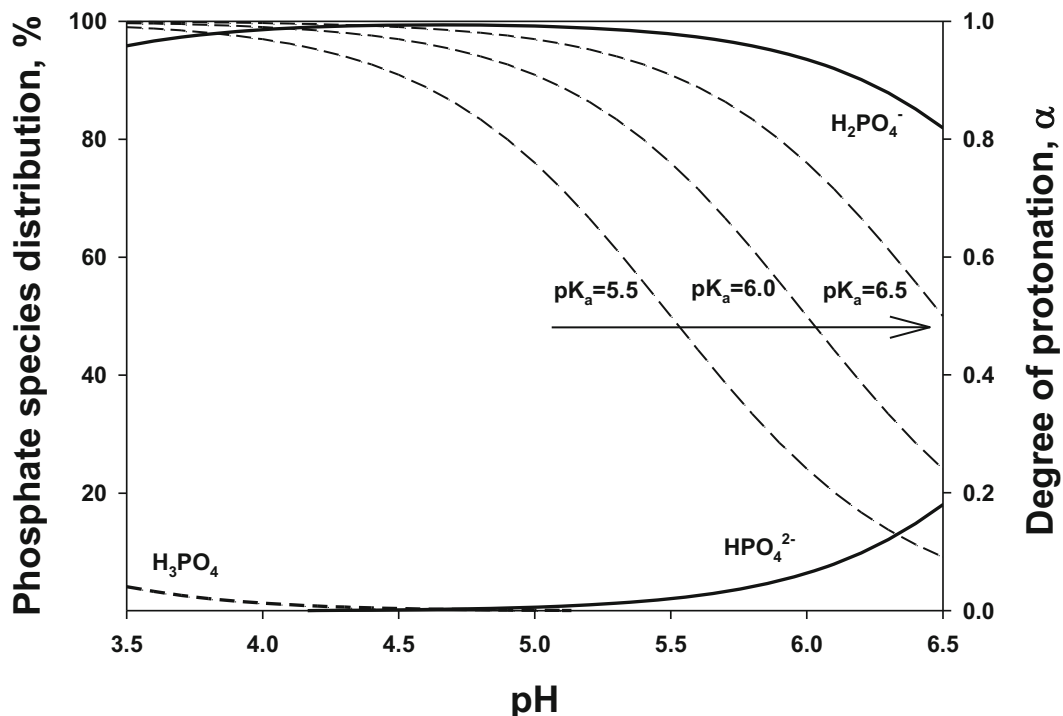


**Fig. 4** Phosphate species distribution and degree of protonation ( $\alpha$ ) as a function of pH



**Fig. 5** Cu(II) (a) and phosphate (b) equilibrium uptakes (symbols: observed data; line: Langmuir model fits)

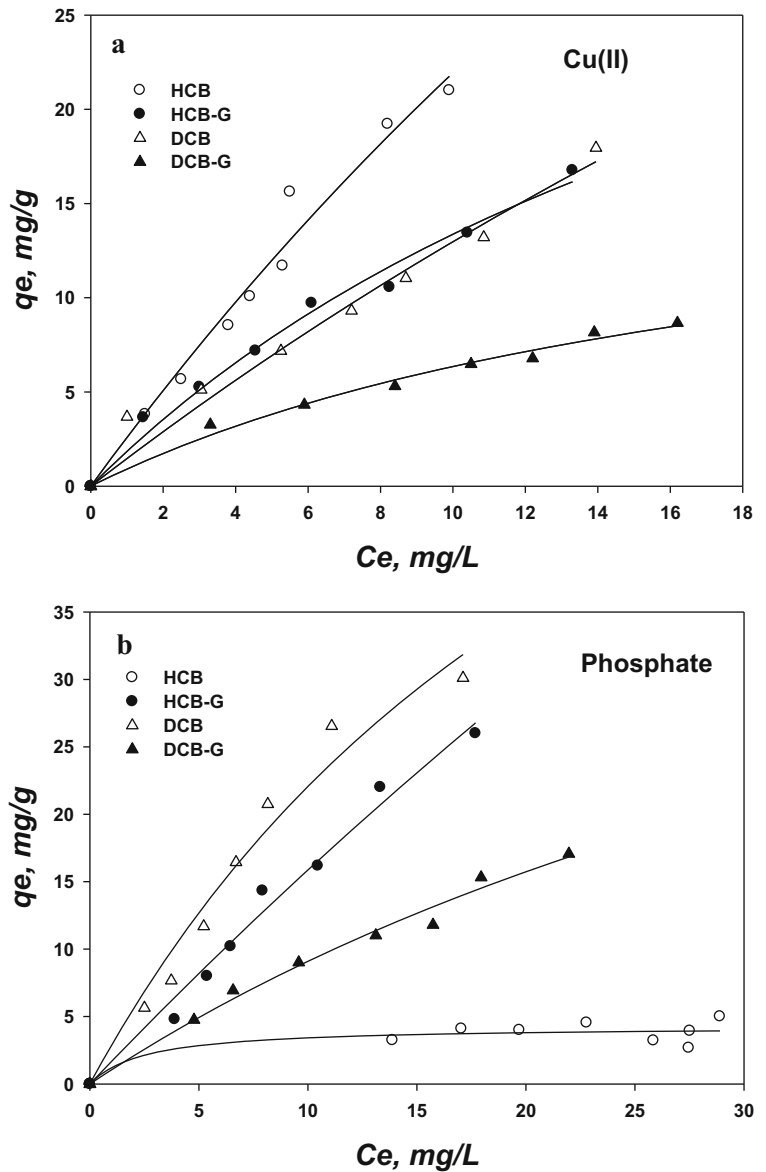
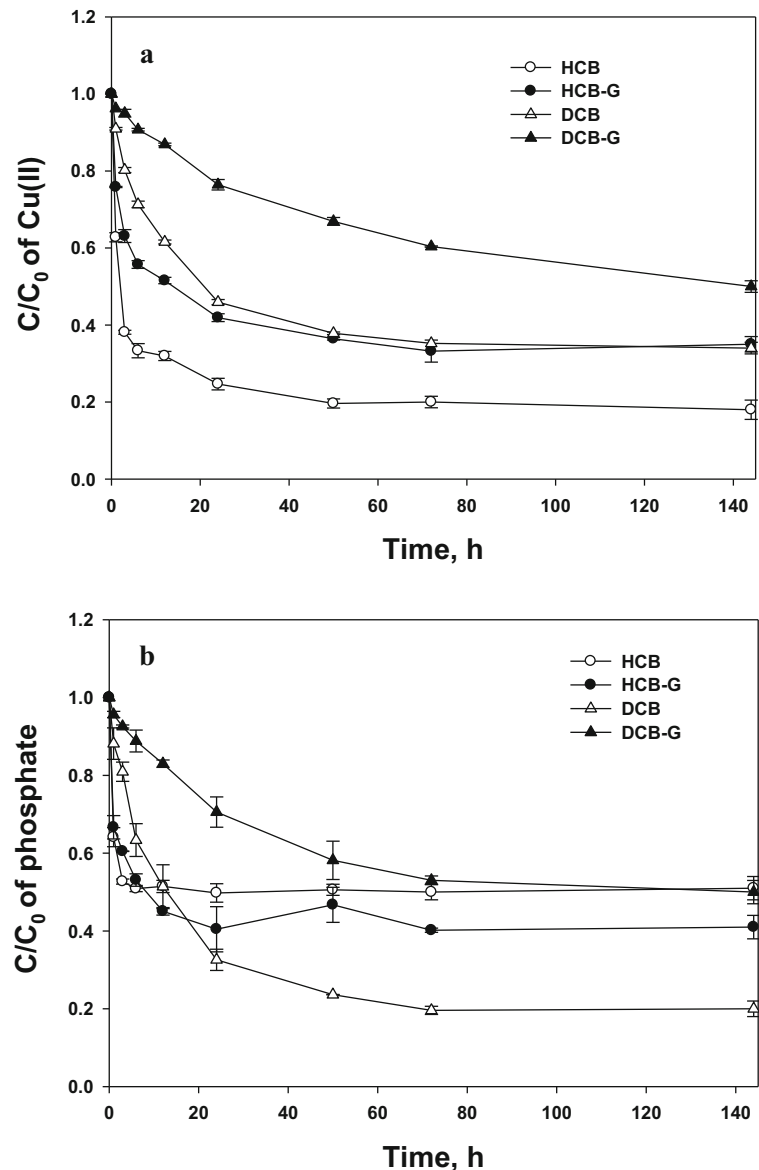


**Table 3** Langmuir ( $Q$ ,  $b$ ) values with  $R^2$

Type of bead	Cu(II)			Phosphate		
	$Q$	$b$	$R^2$	$Q$	$b$	$R^2$
HCB	129 ± 93.5	0.0205 ± 0.0170	0.972	4.19 ± 27.0	0.396 ± 1.14	0.737
HCB-G	43.7 ± 10.4	0.0441 ± 0.0148	0.984	251 ± 254	0.00670 ± 0.00740	0.982
DCB	101 ± 94.8	0.0147 ± 0.0160	0.965	232 ± 238	0.0112 ± 0.0130	0.956
DCB-G	18.9 ± 3.41	0.0508 ± 0.0146	0.984	58.4 ± 19.2	0.0185 ± 0.00790	0.984

**Fig. 6** Cu(II) (a) and phosphate (b) sorption kinetics for the different CBs

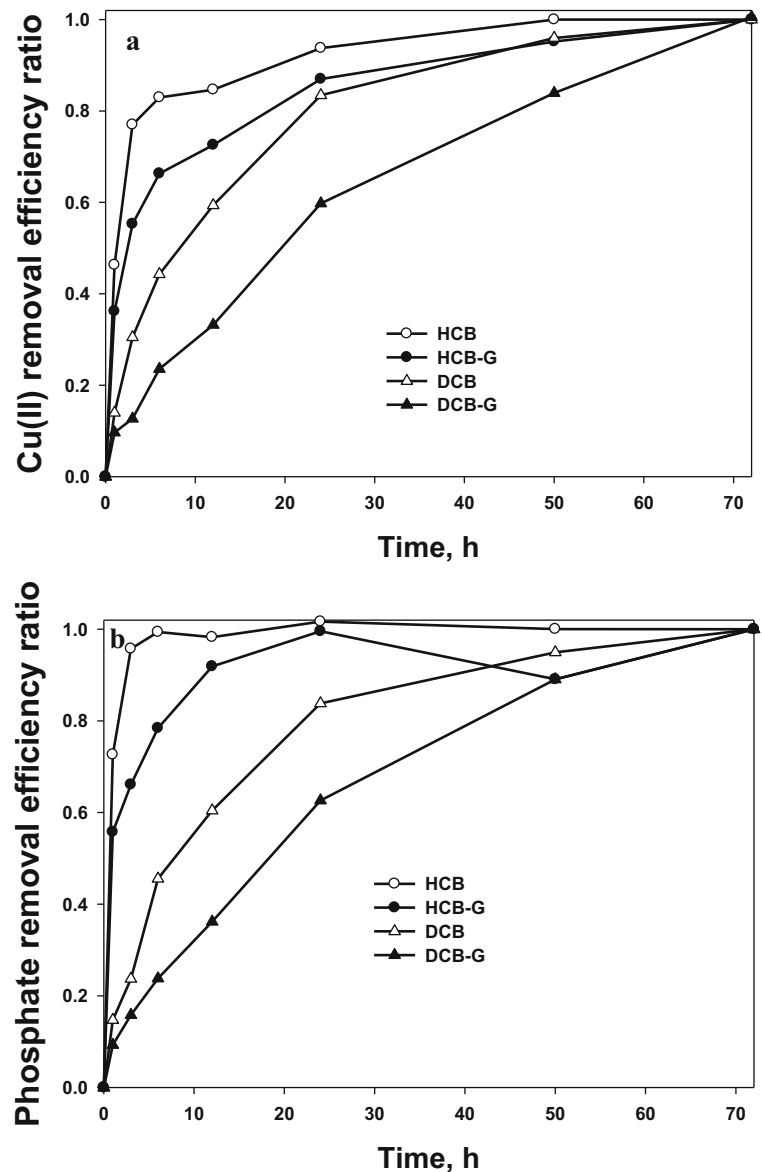


G. For phosphate, the equilibrium sorption rates were 6, 24, 72, and 144 h for HCB, HCB-G, DCB, and DCB-G, respectively. The higher rate for phosphate is in contrast with the findings of Guibal (2004), who stated that the diffusion rate of poly oxo-anions may be reduced by steric hindrance. Kannamba et al. (2010) used chitosan flakes for treating Cu(II), Chiou and Li (2002) crosslinked HCB for treating dye, and Gerente et al. (2010) used chitosan flakes for treating arsenic, and obtained equilibrium sorption rates of 12, 4, and 10 h, respectively. Therefore, the time to complete

sorption was determined under the initial experimental conditions.

To define the effect of crosslinking and drying on the sorption rate, regardless of the sorption capacity, Fig. 7 is re-plotted by the removal ratio of each to total the removal (the time was shown until 72 h). HCB and HCB-G achieved phosphate sorption values of approximately 95% and 65% within 3 h, while Cu(II) sorption reached 75% and 55%, respectively. For both dried beads (DCB and DCB-G), Cu(II) sorption reached approximately 30% and 10%, while that of phosphate

**Fig. 7** Cu(II) (a) and phosphate (b) removal efficiency ratios (each time removal efficiency/total removal efficiency)



reached approximately 25 and 15%, respectively, at 3 h. These values are three to five times lower than those of the hydrogel beads. Like drying, crosslinking also reduced the sorption rate. For hydrogel, the Cu(II) and phosphate decreased by 32–66% and 31–35% within 3 h, respectively.

These observations indicate that crosslinking and drying reduce the sorption rate by reducing the porosity of CB. For example, the application of alginate beads for the removal of Cu(II) showed that the time required by the dried alginate was doubled due to the limitation of intraparticle diffusion by the lack of porosity

(Papageorgiou et al. 2006; An et al. 2014b). Moreover, the crystallinity index was suggested by Piron and Domarda (1998), which restricts molecular mobility in the inner polymer network.

#### 4 Conclusions

Four types of chitosan beads were synthesized and investigated to determine the effect of crosslinking and drying on the simultaneous removal of Cu(II) and phosphate. The type of CB significantly controls the removal

efficiency, and the cation and anion were affected by the physical and chemical modification differently. The highest removal efficiencies of Cu(II) and phosphate were 80% and 60% for HCB and DCB, respectively, and Cu(II) and phosphate removal decreased in the following orders HCB > HCB-G > DCB and DCB > HCB-G > HCB and DCB-G, respectively. Although each uptake was different, the total uptake (mmol) for both Cu(II) and phosphate remained constant, regardless of the type of CB, except for DCB-G due to the degree of protonation of the amino group. The removal efficiency of phosphate was not affected by the initial pH, while that for Cu(II) decreased by approximately 20% below pH 4, corresponding to the species of phosphate and hydrogen completion, respectively. The Langmuir sorption model obtained a maximum Cu(II) level of 129 mg/g by HCB and phosphate level of approximately 250 mg/g by HCB-G or DCB. The sorption rate of the hydrogel bead was higher than that of the dried bead for both the cation and anion, and the sorption rate for phosphate was faster than that for Cu(II).

**Funding Information** This research was supported by Basic Science Research Program through the National Research Foundation of Korea (NRF) funded by the Ministry of Education (No. 2016R1D1A1B03930265) and the Korea Ministry of Environment as a “Global Top Project” (Project No.: 2016002190003). This work was also supported by the Technology Innovation Program (10082572, Development of Low Energy Desalination Water Treatment Engineering Package System for Industrial Recycle Water Production) funded by the Ministry of Trade, Industry & Energy (MOTIE, Korea).

## References

- Agarwal, R., & Gupta, M. N. (1995). Evaluation of glutaraldehyde-modified chitosan as a matrix for hydrophobic interaction chromatography. *Analytica Chimica Acta*, 313, 253–257.
- An, B., Jung, K. Y., Lee, S. H., Lee, S., & Choi, J. W. (2014a). Effective phosphate removal from synthesized wastewater using copper-chitosan bead: batch and fixed-bed column studies. *Water Air Soil Pollution*, 225, 2050.
- An, B., Jung, K. Y., Zhao, D., Lee, S. H., & Choi, J. W. (2014b). Preparation and characterization of polymeric ligand exchanger based on chitosan hydrogel for selective removal of phosphate. *Reactive and Functional Polymers*, 85, 45–53.
- Cegłowski, M., Gierczyk, B., Frankowski, M., & Popenda, L. (2018). A new low-cost polymeric adsorbents with polyamine chelating groups for efficient removal of heavy metal ions from water solutions. *Reactive and Functional Polymers*, 131, 64–74.
- Chang, X., Chen, D., & Jiao, X. (2008). Chitosan-based aerogels with high adsorption performance. *Journal of Physical Chemistry B*, 112(26), 7721–7725.
- Chen, F., Wu, Q., Lü, Q., Xu, Y., & Yu, Y. (2015). Synthesis and characterization of bifunctional mesoporous silica adsorbent for simultaneous removal of lead and nitrate ions. *Separation and Purification Technology*, 151, 225–231.
- Chiou, M. S., & Li, H. Y. (2002). Equilibrium and kinetic modeling of adsorption of reactive dye on cross-linked chitosan bead. *Journal of Hazardous Materials*, 93, 233–248.
- Conley, D. J., Paerl, H. W., Howarth, R. W., Boesch, D. F., Seitzinger, S. P., Havens, K. E., Lancelot, C., & Likens, G. E. (2009). Controlling eutrophication: Nitrogen and phosphorus. *Science*, 323, 1014–1015.
- Denizli, A., Say, R., Patr, S., & Arica, M. Y. (2000). Adsorption of heavy metal ions onto ethylene diamine-derived and cibacron blue F3GA-incorporated microporous poly(2-hydroxyethyl methacrylate) membranes. *Reactive functional Polymers*, 43, 17–24.
- Domard, A. (1987). Determination of N-acetyl content in chitosan samples by c.d. measurements. *International Journal of Biological Macromolecules*, 9, 333–336.
- Gerente, C., Andres, Y., McKay, G., & Le Cloirec, P. (2010). Removal of arsenic(V) onto chitosan: From sorption mechanism explanation to dynamic water treatment process. *Chemical Engineering Journal*, 158, 593–598.
- Guibal, E. (2004). Interactions of metal ions with chitosan-based sorbents: A review. *Separation and Purification Technology*, 38, 43–74.
- Guibal, E., Milot, C., & Tobin, J. M. (1998). Metal-anion sorption by chitosan beads: Equilibrium and kinetic studies. *Industrial and Engineering Chemistry Research*, 37, 1454–1463.
- He, Y., Lin, H., Dong, Y., Liu, Q., & Wang, L. (2016). Simultaneous removal of ammonium and phosphate by alkaline-activated and lanthanum-impregnated zeolite. *Chemosphere*, 164, 387–395.
- Hu, Y. N., & Cheng, H. F. (2013). Water pollution during China’s industrial transition. *Environmental Development*, 8, 57–73.
- Ishii, T., Sorita, A., Sawamura, M., Kusunose, H., & Ukeda, H. (1997). Determination of the reaction-product of glutaraldehyde and amine based on the binding ability of Coomassie brilliant blue. *Analytical Sciences*, 13, 5–9.
- Jabli, M., Baouab, M. H. V., Sintès-Zydowicz, N., & Hassine, B. B. (2011). Dye molecules/copper(II)/macroporous glutaraldehyde-chitosan microspheres complex: Surface characterization, kinetic, and thermodynamic investigations. *Journal of Applied Polymer Science*, 123, 3412–3424.
- Jo, H. J., Choi, J. W., Lee, S. H., & Hong, S. W. (2012). Acute toxicity of Ag and CuO nanoparticle suspensions against *Daphnia magna*: The importance of their dissolved fraction varying with preparation methods. *Journal of Hazardous Materials*, 227–228, 301–308.
- Kannamba, B., Reddy, K. L., & AppaRao, B. V. (2010). Removal of Cu(II) from aqueous solutions using chemically modified chitosan. *Journal of Hazardous Materials*, 175, 939–948.
- Kildeeva, N. R., Perminov, P. A., Vladimirov, L. V., Novikov, V. V., & Mikhailov, S. N. (2009). About mechanism of chitosan cross-linking with glutaraldehyde. *Russian Journal of Bioorganic Chemistry*, 35(3), 397–407.
- Kim, H., Choi, J. W., Kim, T. H., Park, J. S., & An, B. (2018). Effect of TSS removal from stormwater by mixed media

- column on T-N, T-P, and organic material removal. *Water*, 10(8), 1069.
- Li, B., Shan, C. L., Zhou, Q., Fang, Y., Wang, Y. L., Xu, F., Han, L. R., Ibrahim, M., Guo, L. B., Xie, G. L., & Sun, G. C. (2013). Synthesis, characterization, and antibacterial activity of cross-linked chitosan-glutaraldehyde. *Marine Drugs*, 11, 1534–1552.
- Liu, X., & Zhang, L. (2015). Removal of phosphate anions using the modified chitosan beads: Adsorption kinetic, isotherm and mechanism studies. *Powder Technolog*, 277, 112–119.
- Liu, Y., Yan, C., Zhao, J., Zhang, Z., Wang, H., Zhou, S., & Wu, L. (2018). Synthesis of zeolite P1 from fly ash under solven-free conditions for ammonium removal from water. *Journal of Cleaner Production*, 202, 11–22.
- Malwal, D., & Gopinath, P. (2017). Silica stabilized magnetic-chitosan beads for removal of arsenic from water. *Colloid and Interface Science Communications*, 19, 14–19.
- Modrezejewska, Z. (2013). Sorption mechanism of copper in chitosan hydrogel. *Reactive Functional Polymers*, 73, 719–726.
- Monteiro Jr., O. A. C., & Airoidi, C. (1999). Some studies of crosslinking chitosan–glutaraldehyde interaction in a homogeneous system. *International Journal of Biological Macromolecules*, 26, 119–128.
- Noel, S. P., Courtney, H. S., Bumgardner, J. D., & Haggard, W. O. (2010). Chitosan sponges to locally deliver amikacin and vancomycin: A pilot in vitro evaluation. *Clinical Orthopaedics and Related Research*, 468(8), 2074–2080.
- Osman, Z., & Arof, A. K. (2003). FTIR studies of chitosan acetate based polymer electrolytes. *Electrochimica Acta*, 48, 993–999.
- Papageorgiou, S. K., Katsaros, F. K., Kouvelos, E. P., Nolan, J. W., Le Deit, H., & Kanellopoulos, N. K. (2006). Heavy metal sorption by calcium alginate beads from *Laminaria digitata*. *Journal of Hazard Materials*, 137(3), 1765–1772.
- Pillai, C. K. S., Paul, W., & Sharma, C. P. (2009). Chitin and chitosan polymers: Chemistry, solubility and fiber formation. *Progress in Polymer Science*, 34(7), 641–678.
- Piron, E., & Domarda, A. (1998). Interaction between chitosan and uranyl ions. Part 2. Mechanism of interaction. *International Journal of Biological Macromolecules*, 22(1), 33–40.
- Poon, L., Wilson, L. D., & Headley, J. V. (2014). Chitosan-glutaraldehyde copolymers and their sorption properties. *Carbohydrate Polymers*, 109, 92–101.
- Queiroz, M. F., Melo, K. R. T., Sabry, D. A., Sasaki, G. L., & Rocha, H. A. O. (2015). Does the use of chitosan contribute to oxalate kidney stone formation? *Marine Drugs*, 13, 141–158.
- Rajeswari, A., Amalraj, A., & Pius, A. (2015). Removal of phosphate using chitosan-polymer composites. *Journal of Environmental Chemical Engineering*, 3, 2331–2341.
- Sampaio, R. M. M., Timmers, R. A., Xu, Y., Keesman, K. J., & Lens, P. N. L. (2009). Selective precipitation of cu from Zn in a Ps controlled continuously stirred tank reactor. *Journal of Hazardous Materials*, 165, 256–265.
- Schindler, D. W. (1974). Eutrophication and recovery in experimental lakes: Implications for lake management. *Science*, 184, 897–899.
- Shah, B., & Chudasama, U. (2014). Synthesis and characterization of a novel hybrid material as amphoteric ion exchanger for simultaneous removal of cations and anions. *Journal of Hazardous Materials*, 276, 138–148.
- Sorvari, J., & Sillanpää, M. (1996). Influence of metal complex formation on heavy metal and free EDTA and DTPA acute toxicity determined by *Daphnia magna*. *Chemosphere*, 33(6), 1119–1127.
- Stoll, A., & Duncan, J. R. (1996). Enhanced heavy metal removal from waste water by viable, glucose pretreated *Saccharomyces cerevisiae* cells. *Biotechnology Letters*, 18(10), 1209–1212.
- Thakur, V. K., & Voicu, S. I. (2016). Recent advances in cellulose and chitosan based membranes for water purification: A concise review. *Carbohydrate Polymers*, 146, 148–165.
- USEPA, EPA440/5–86-001, Washington, DC, 1986.
- Verbych, S., Bryk, M., Chornokur, G., & Fuhr, B. (2005). Removal of copper (II) from aqueous solutions by chitosan adsorption. *Separation Science and Technology*, 40, 1749–1759.
- Wan Ngah, W. S., Endud, C. S., & Mayanar, R. (2002). Removal of copper(II) ions from aqueous solution onto chitosan and cross-linked chitosan beads. *Reactive and Functional Polymer*, 50(2), 181–190.
- Wang, Q. Z., Chen, X. G., Liu, N., Wang, S. X., Liu, C. S., Meng, X. H., & Liu, C. G. (2006). Protonation constants of chitosan with different molecular weight and degree of deacetylation. *Carbohydrate Polymers*, 65, 194–201.
- Wang, J. J., Zeng, Z. W., Xiao, R. Z., Xie, T., Zhou, G. L., Zhan, X. R., & Wang, S. L. (2011). Recent advances of chitosan nanoparticles as drug carriers. *International Journal of Nanomedicine*, 6, 765–774.
- Wu, Q., Chen, F., Xu, Y., & Yu, Y. (2015). Simultaneous removal of cations and anions from waste water by bifunctional mesoporous silica. *Applied Surface Science*, 351, 155–163.
- Xie, Y. L., Wang, M. J., & Yao, S. J. (2009). Preparation and characterization of biocompatible microcapsules of sodium cellulose sulfate/chitosan by means of layer-by-layer self-assembly. *Langmuir*, 25(16), 8999–9005.
- Zhao, F., Yu, B., Yue, Z., Wang, T., Wen, X., Liu, Z., & Zhao, C. (2007). Preparation of porous chitosan gel beads for copper(II) ion adsorption. *Journal of Hazardous Materials*, 147, 67–73.